URTeC: 4244384

Fracture Conductivity, Proppant Loading, and Well Performance in the Bakken

Craig Cipolla*[1], Michael McKimmy[1], John Lassek[1], Sama Morsy[2], Mark McClure[2]
1. Hess Corporation, 2. ResFrac Corporation.

This paper was prepared for presentation at the Unconventional Resources Technology Conference held in Houston, Texas, USA, 9-11 June 2025.

Abstract

This paper leverages a comprehensive dataset of drainage measurements from four observation lateral projects in the Bakken to rigorously characterize conductivity along the hydraulic fracture length and drainage as a function of distance away from the lateral. These drainage mapping projects also included fiber optic measurements of completion effectiveness (completion well distributed acoustic sensing or DAS), fracture morphology (offset well distributed strain sensing or DSS) and microseismic data, providing a complete dataset to evaluate fracture geometry. The first drainage mapping project was published by Cipolla et. al. (2022), with two more projects published by McKimmy et. al. (2025). Additional insights were published by Liang et. al. (2022).

A fully coupled hydraulic fracture and reservoir simulation model was calibrated to match this comprehensive fracture geometry, drainage, and well performance dataset. The model calibration is summarized in the paper. The calibrated model was used to evaluate the impact of proppant loading and treatment size on well productivity and ultimate oil recovery for well spacing of 500, 770, and 1080 ft. Average proppant loading was varied from an average of 0.6 lbs of proppant added per gallon of fluid (PPA) to 2 PPA. And jobs sizes representing standard, large, and very large treatment volumes were modeled. Slickwater fluids and typical proppant schedules were used for all simulations.

Typical slickwater treatments utilize an average proppant concentration of about 1 PPA (total lbs proppant/total gallons of fluid) and there has been little focus on the impact of higher proppant concentrations on well productivity and oil recovery. This paper provides new insights into the impact of proppant concentration on well productivity and oil recovery in the Bakken.

The drainage measurements showed that fracture conductivity in the Bakken is low, and drainage is limited to about 50% of the fracture half-length. Fracture conductivity and drainage may be adequate in the first 25% of the productive half-length, but drainage is materially impeded in the second 25% of the productive half-length due to very low fracture conductivity. The modeling indicated that increasing proppant loading improved well productivity and ultimate recovery for all treatments sizes and well spacing evaluated. However, there were diminishing incremental increases in well productivity and oil recovery as treatment size increased, especially for the 500 and 770 ft well spacing. A detailed economic analysis was performed and the normalized results presented in the paper.

Introduction

Until recently, accurately characterizing fracture conductivity and drainage has been difficult due to an absence of direct measurements. This paper focuses on the Bakken formation and builds on a unique dataset that provided direct measurements of drainage as a function of distance and treatment designs. Cipolla et. al. (2022) showed that Middle Bakken (MB) wells could drain the underlying Three Forks (TF) formation at a distance of 450 ft and that treatment design could significantly affect drainage efficiency. This work also provided important insights into the relationship between fracture length and treatment volume, and fracture morphology as a function of distance from the treatment well. Liang et. al. (2022) presented direct measurements of MB drainage as a function of distance from the treatment well. McKimmy et. al. (2025) provided additional insights into MB drainage (fixed distance) and MB-TF drainage (variable distances).

Drainage efficiency as a function of distance along the fracture azimuth after 1-year of production is shown in **Figure 1** [Cipolla et. al., 2024], summarizing the learnings for multiple Bakken drainage mapping projects. Although the drainage curves are shown after 1-year of production, longer term measurements suggest the 1-year data is representative of long-term drainage efficiency. The y-axis shows the depletion in the hydraulic fracture after 1-year of production, presented as a percentage of the initial reservoir

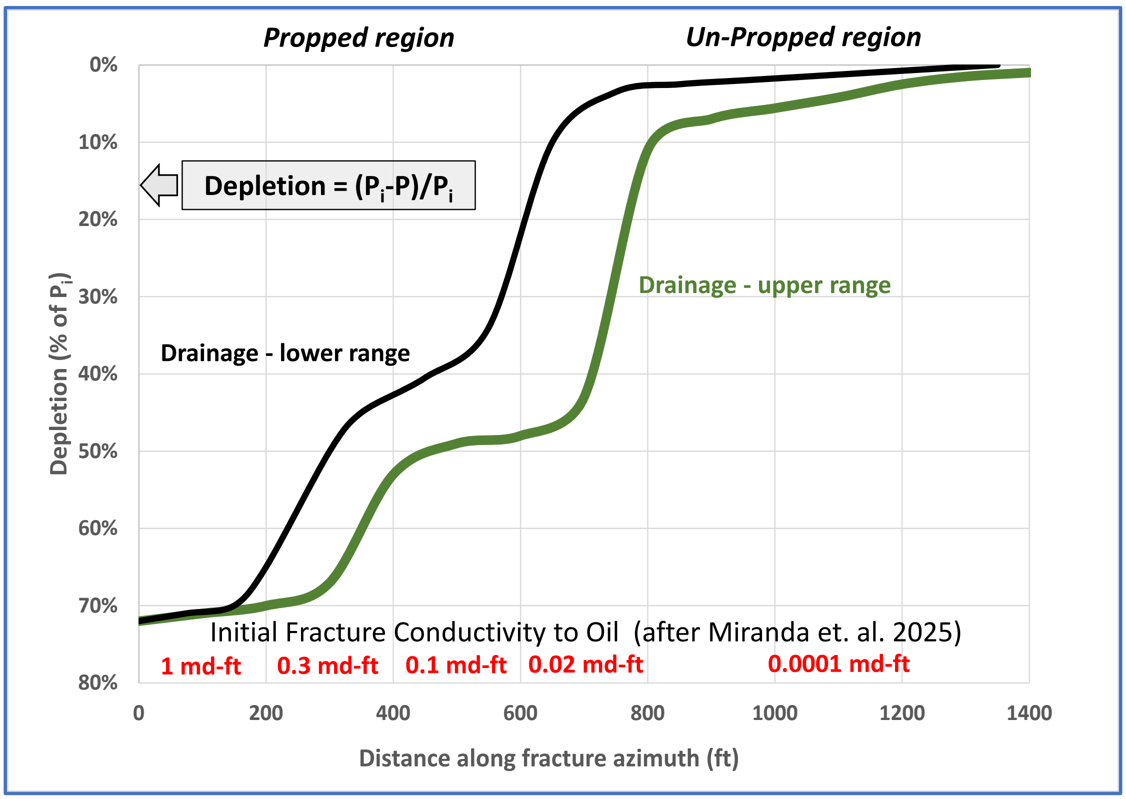

Figure 1 - Drainage efficiency as a function of distance along the fracture azimuth, Fig. 18, Cipolla et. al. (2024)

pressure. For example, assuming an original reservoir pressure in the Bakken of 7000 psi, if the measured pressure at a given distance is 4000 psi then the depletion would be 43% [(7000-4000)/7000]. The figure shows a lower and upper range for drainage that is characteristic of the variation in drainage as a function of treatment design (e.g. – treatment size, proppant type, proppant loading) and lateral position (e.g., MB-MB or MB-TF drainage). For example, the lower drainage curve could be representative of MB-TF drainage using standard treatment sizes or MB-MB drainage using small treatments.

There are three distinct drainage regions shown in Figure 1, representing good, moderate, and poor drainage. The region of the hydraulic fracture with poor drainage is likely un-propped. Basic proppant transport theory using slickwater fluids (Msalli and Miskimins, 2020) would predict that more proppant and larger proppant is placed near the wellbore, while less proppant and smaller proppant is transported farther in the fracture, consistent with the good and moderate drainage regions (i.e. – propped fracture). The figure shows that drainage is relatively good within 200-300 ft of the wellbore. However, drainage is much less effective at distances of 300-700 ft (moderate drainage). While total fracture lengths can be 1000-1400 ft or longer, effective drainage is limited to 500-700 ft or about 50% of the fracture length. There is poor drainage beyond 700 ft, with less than a 10% decrease in initial reservoir pressure after 1-year of production. These comprehensive drainage and fracture geometry and fracture morphology measurements provided a rich dataset to characterize fracture conductivity and calibrate hydraulic fracture and reservoir simulation models.

Miranda et. al. (2025) performed a detailed modeling study using a ¼-fracture model to characterize fracture conductivity by history matching the production behavior **and** drainage measurements used to develop the curves shown in Figure 1. The results from this study are shown along the x-axis in Figure 1, illustrating that the initial fracture conductivity to oil near the wellbore is about 1 md-ft and decreases dramatically along the fracture length. The conductivity to oil is about 0.02 md-ft in the transition region between the propped and un-propped areas of the hydraulic fracture (600-800 ft), while the drainage beyond 800 ft was matched using an initial conductivity of 0.0001 md-ft. The conductivity to oil is about 5% of the total fracture conductivity and decreases substantially as closure stress (drawdown) increases. The drastic decreases in fracture conductivity due to multi-phase flow, non-Darcy flow, and closure stress are discussed in detail by Palisch et. al. (2007).

Model Calibration

A unique aspect of this work was the opportunity to utilize comprehensive and diverse datasets of direct measurements of drainage, fracture geometry, fracture morphology, and far-field fracture propagation pressures to calibrate a fully coupled hydraulic fracture and reservoir simulation model. The fully coupled hydraulic fracture and reservoir simulation model used for this study is described by McClure et. al. (2024a, 2024b). An in-depth discussion of the model calibration is beyond the scope of the paper, but the results will be summarized. Details of the model calibration using the dataset presented by Cipolla et. al. (2022) are provided by McClure et. al. (2023) and Singh et. al. (2025), referenced as dataset BK1 in both papers. This dataset documented MB-TF drainage at a fixed distance for three different fracture treatment designs, while also providing fracture length as function of treatment volume and fracture morphology as a function of distance.

Singh et. al. (2025) also presents a discussion of the model calibrations and workflow for a Bakken dataset measuring drainage as function of distance along the hydraulic fracture length as reported by Liang et. al. (2022). This Bakken dataset is referenced as BK2 and illustrates how drainage efficiency decreases dramatically as distance away from the wellbore increases. The conclusions from this work highlighted the low fracture conductivity and limited drainage characteristic of these Bakken datasets, consistent with the results presented by Miranda et. al. (2025). This same workflow was applied to extend the model calibrations using the measurements from two additional projects showing MB-MB drainage at a fixed distance and MB-TF drainage at a variable distance (McKimmy et. al. 2025).

An example of the fracture geometry and morphology from the calibrated model is shown in **Figure 2**, using the dataset presented by Cipolla et. al. (2022). Note that the modeling was performed using a sector model. In this example seven clusters per stage and six child wells were modeled. The morphology illustrated in Figure 2 shows 70% of the fractures initiated at the wellbore propagate 550 ft, while only 57% reach 1100 ft and just 14% extend to 1650 ft. The fracture lengths and morphology from the calibrated model are representative of the measurements documented by Cipolla et. al. (2022).

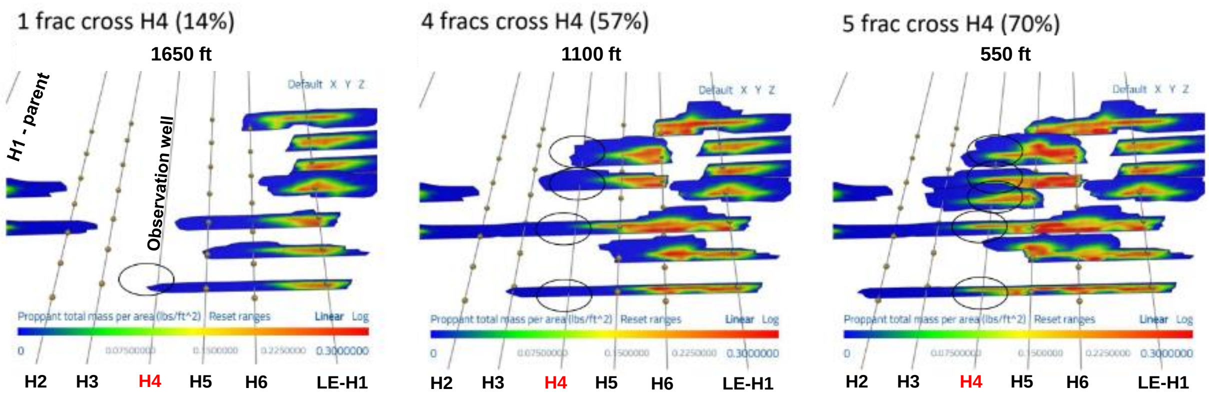

Figure 2 - Example of fracture geometry and morphology using Bakken dataset BK1 (Cipolla et. al. 2022)

In the BK1 dataset, three treatment designs were evaluated in the H3 and H5 wells and the impact on drainage measured in the H4 observation well. The treatments were pumped in ~2000 ft offsetting sections in the H3 and H5 laterals and tracers were used to compare the production. Additional details are provided by Cipolla et. al. (2022). The calibrations were extended to ensure the model accurately captured the effect of treatment design on production and drainage. **Figure 3** shows the oil tracer measurements that suggest Designs 2 and 3 substantially out-performed Design 1, with Design 3 producing 40% more oil (left-side bar chart). The calibrated model accurately reproduced this behavior (Figure 3, right-side graphic).

The next step in the calibration process was to ensure that the model reliably predicted drainage as a function of distance and treatment design. **Figure 4** compares the predicted drainage behavior for Designs 1, 2, and 3, as discussed above. The differences in drainage as a function of treatment design are consistent with the measurements presented by Cipolla et. al.,2022 (ref. Figure 20). Figure 4 also compares the predicted drainage as a function of distance for relatively large treatment volumes at distances of 300 ft, 600 ft, 900 ft, and 1200 ft along the frac length, showing good agreement with the drainage curves. **Figure 5** shows an example of the model-predicted drainage using MB and TF observation wells at the above distances. The

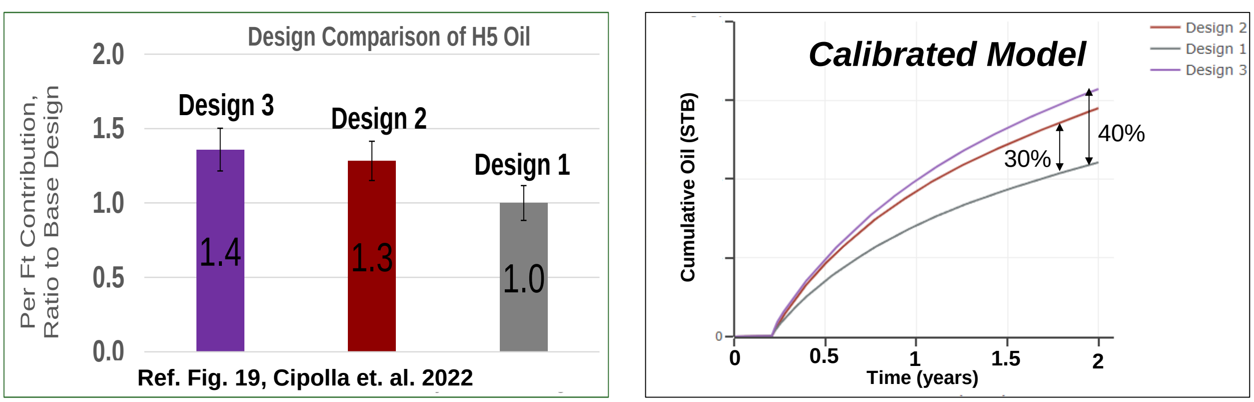

Figure 3 - Effect of treatment designs on well productivity, calibrated model, and actual results.

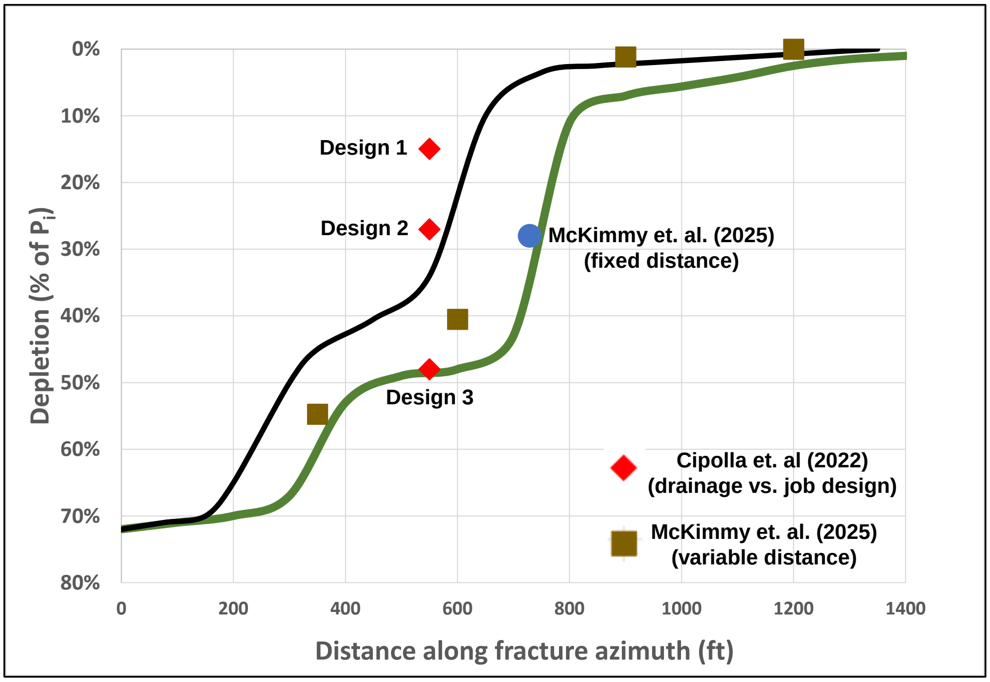

Figure 4 - Comparison of drainage curves and model-predicted drainage.

model drainage varies depending on the proppant distribution in each fracture and observation well location (MB or TF) and the variability is consistent with the field measurements (Cipolla et. al. 2022, McKimmy et. al. 2025). The average model-predicted drainage is presented for simplicity. For reference, McKimmy et. al. (2025) show drainage versus distance using six gauges that span drainage distances of 560 ft to 1240 ft; these measurements supported the development of the drainage curves.

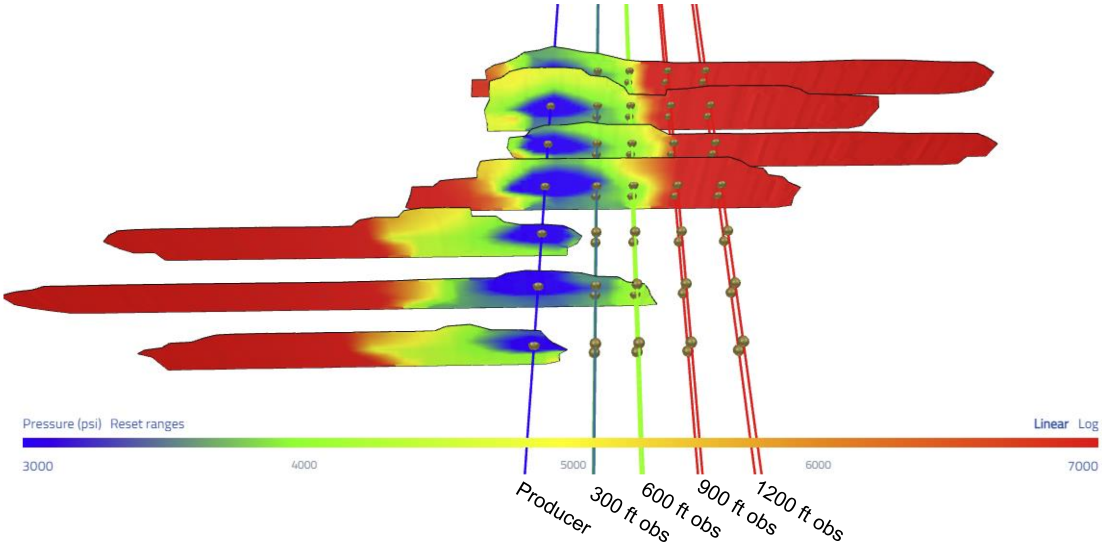

Figure 5 - Example of model-predicted drainage using eight observation wells (4 MB and 4 TF)

McKimmy et. al. (2025) also document drainage measurements from 16 gauges placed at a fixed distance of about 750 ft along the fracture azimuth from the primary drainage well (two-well pad with an observation well in between). The basic layout of this project is shown in **Figure 6a**. Note that the primary completion well is 620 ft from the observational lateral, which is about 750 ft along the N55E fracture azimuth. Very large treatment volumes were pumped in the primary completion well (H5), while standard treatment volumes were pumped in the LE-H1. In addition, the LE-H1 well had 25% more perforation clusters than the H5 well. These differences in completion design were intended to bias the observation well measurements to reflect the H5 drainage. This dataset provided a unique opportunity to validate the calibrated model using a relatively simple two-well “system.” In addition, the observation lateral was completed about one year after the outer wells were put-on-production, providing a very important second validation of the model calibrations.

Figure 6b shows excellent agreement between the predicted and actual oil production for the two outer wells; the GOR and water cut were also matched. BHP measurements were available on one of the wells, while BHP was calculated from surface pressure for the other well (and used to control the model). The predicted drainage after one year of production from the two outer wells is shown in Figure 5 (blue dot) and is in good agreement with the actual measurements (McKimmy et. al. 2025). **Figure 6c** shows the predicted pad oil production after the completion of the observation lateral and is in good agreement with the actual oil production, although slightly over-predicting the production. The calibrated model accurately predicted that the completion of the observation lateral would not materially increase pad-level oil production due to the drainage from the offset wells, providing a final validation of the model calibrations.

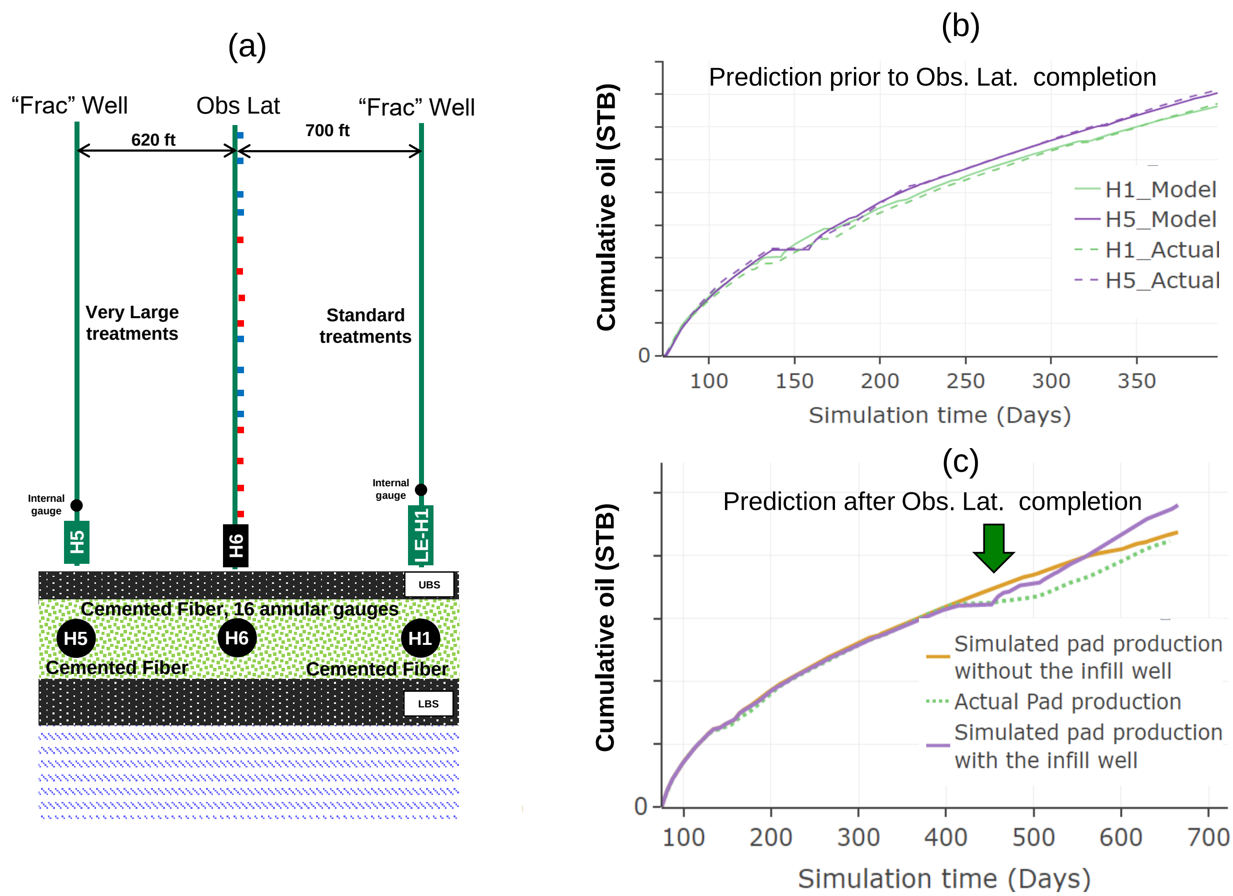

Figure 6 - Drainage measurements at a fixed distance, after McKimmy et. al. 2025 (a), comparison of model-predicted and actual oil production (b), comparison of model-predicted and actual infill well oil production

Summary of Model Calibration

The calibration process integrated multiple surveillance data, including microseismic, cemented gauges, tracers, fiber, and downhole perforation imaging to match:

- fracture geometries; height, length, and asymmetry.
- fracture treatment data; net pressure, wellhead treating pressure, ISIP, cluster efficiency.
- pressure drop along the frac length.
- oil, water, and gas production volumes per well, frac design, and depletion level.
- pressure interference between wells.

The fracture geometry and model calibrations were consistent throughout all the drainage predictions; however, PVT and basic reservoir and geologic properties were adjusted based on the location of each project. The primary calibrations focused on the fracture geometry, proppant, transport, and in situ fracture conductivity. The offset well pressure gauges provided direct measurements of fracture propagation pressures, as all gauges were intersected by hydraulic fractures. These far-field pressure measurements, combined with treatment data and fracture geometry measurements, provided a rare opportunity to calibrate the pressure loss along the fracture length and the fracture growth rate.

The drainage pressures were matched by adjusting the proppant transport parameters, primarily proppant trapping. Proppant trapping parameters were adjusted based on proppant size, with less trapping for smaller proppants or more trapping for larger proppants. Smaller proppant is transported farther than larger proppant, consistent with basic proppant transport theory with additional stratification due to proppant trapping. Details of the proppant trapping parameters are provide by McClure et. al. (2024a, 2024b) and discussed by Singh et. al. (2025) for the BK1 and BK1 datasets. The initial fracture conductivity and decrease in conductivity as closure stress increases and with time were also important calibration parameters.

The direct measurements of drainage and results from this model calibration work, the Bakken modeling presented by Singh et. al. (2025), and the Bakken modeling presented by Miranda et. al. (2025) indicate that fracture conductivity in the Bakken is low. The drainage curves developed using these measurements show that there is significant opportunity to improve drainage and well productivity if conductivity can be increased in the farther regions of the propped fracture (e.g. – from 300 ft to 700 ft), which is this focus of this study. However, there is an even greater opportunity to transform Bakken development if drainage can be extended beyond 800 ft and include most of the created fracture length.

Proppant Loading and Well Performance

Modeling the impact of treatment designs on well performance is relatively easy, but the results would be very unreliable and could possibly lead to poor design choices if the model is not properly calibrated with sufficient measurements. Therefore, a significant portion of this work was dedicated to calibrating the hydraulic fracture and reservoir simulation model to maximize the benefits from the modeling study. The calibrated model was used to evaluate the impact of proppant loading on well performance and drainage. In this study, proppant loading is defined as the pounds of proppant pumped divided by the total fluid volume, including the pad volume (lbs proppant added per gal of fluid, designated PPA). The details of the proppant scheduling are beyond the scope of this paper, but typically proppant scheduling was using in the modeling. A secondary focus of this work was to evaluate the impact of treatment size and proppant loading on well performance and drainage.

The model consisted of three MB wells and observation wells to report MB and TF drainage. The cluster spacing was held constant at 34 ft, with seven clusters and one stage. **Figure 7a** shows the model configuration that was used for the sensitivity study. Three producers were modeled with two observation wells halfway between the producers used to measure drainage effectiveness.

Figure 7b shows a matrix of cases that were evaluated. The base treatment (Job) designs used different average proppant loadings, with standard treatment sizes averaging 1 lbs proppant added per gallon of fluid (1 PPA). The base design for the large and very large treatments utilized lower average proppant loadings of 0.74 PPA and 0.66 PPA, respectively. The different base designs reflected the operator's completion standards prior to this study, with standard jobs used for "standard" well spacing, large jobs used for "large" well spacing, and very large jobs used for "very large" well spacing. However, when evaluating higher proppant loadings, the average concentrations are the same for all job sizes. Although the details of the treatment designs are proprietary, there is a 3x difference in treatment volume and an 2x difference in proppant from the standard to the very large job (Base PPA jobs). All cases used a typical slickwater fluid, consistent with the fluid used during the model calibration process. In addition, all designs used 50% 100-mesh and 50% 40/70-mesh high quality white sand.

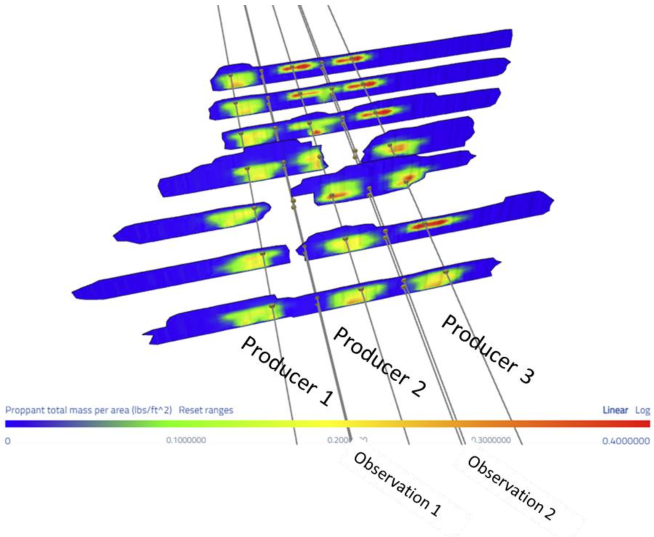

(a)

Well spacing (E-W)	Job Size	Base PPA	PPA2	PPA3	PPA4
500 ft	Standard	0.99			
	Large	0.74			
	Very Large	0.66			
770 ft	Standard	0.99	1.2	1.5	2.0
	Large	0.74	1.2	1.5	2.0
	Very Large	0.66	1.2	1.5	2.0
1080 ft	Standard	0.99			
	Large	0.74			
	Very Large	0.66			

(b)

Figure 7 – Three well model with two observation wells used for the sensitivity study (a) and cases modeled (b)

Drainage efficiency, job design, and well spacing

Figure 8 shows the drainage efficiency for the three job sizes and E-W Bakken well spacings of 500, 770, and 1080 ft (N-S lateral orientation). The fracture lengths are shown on the x-axis, corresponding to the on-azimuth mid-point of well spacing. For example, the mid-point for 1080 ft well spacing is 540 ft, requiring a fracture length of about 700 ft (N50E azimuth) to drainage that E-W distance. The base case PPA results (left graphs) show that standard job sizes provide good MB and TF drainage for 500 ft well spacing and increasing job size does not improve drainage. As well spacing increases, the impact of job size becomes more evident. At 770 ft well spacing, large jobs show about 7% more drainage in the MB and 21% more TF drainage compared to the standard job size. However, very large jobs do not improve drainage efficiency at 770 ft well spacing. The benefit of very large jobs is seen at 1080 ft well spacing, with drainage efficiency of about 40-45% compared to 10-30% for the large treatments.

The graphics shown on the right side of Figure 8 provide drainage efficiency for an average proppant loading of 1.5 PPA and well spacing of 770 ft. Increasing the average PPA to 1.5 improves MB drainage by about 8% and TF drainage by about 24% for the standard job size. Note that the treatment volumes are not changed for the three job sizes, only the average proppant loading in changed. There is about 5% difference in MB and TF drainage efficiency between the standard and very large job volumes when increasing proppant loading to 1.5 PPA, suggesting that standard treatment "volumes" may provide adequate drainage at 770 ft well spacing when proppant loading is increased to 1.5 PPA. The results emphasize the complex trade-off between fluid volume, proppant loading, and drainage efficiency. In some cases, smaller treatment volumes with higher proppant loading may provide the best results. A comparison of the economics of the various job designs is provided later in the paper.

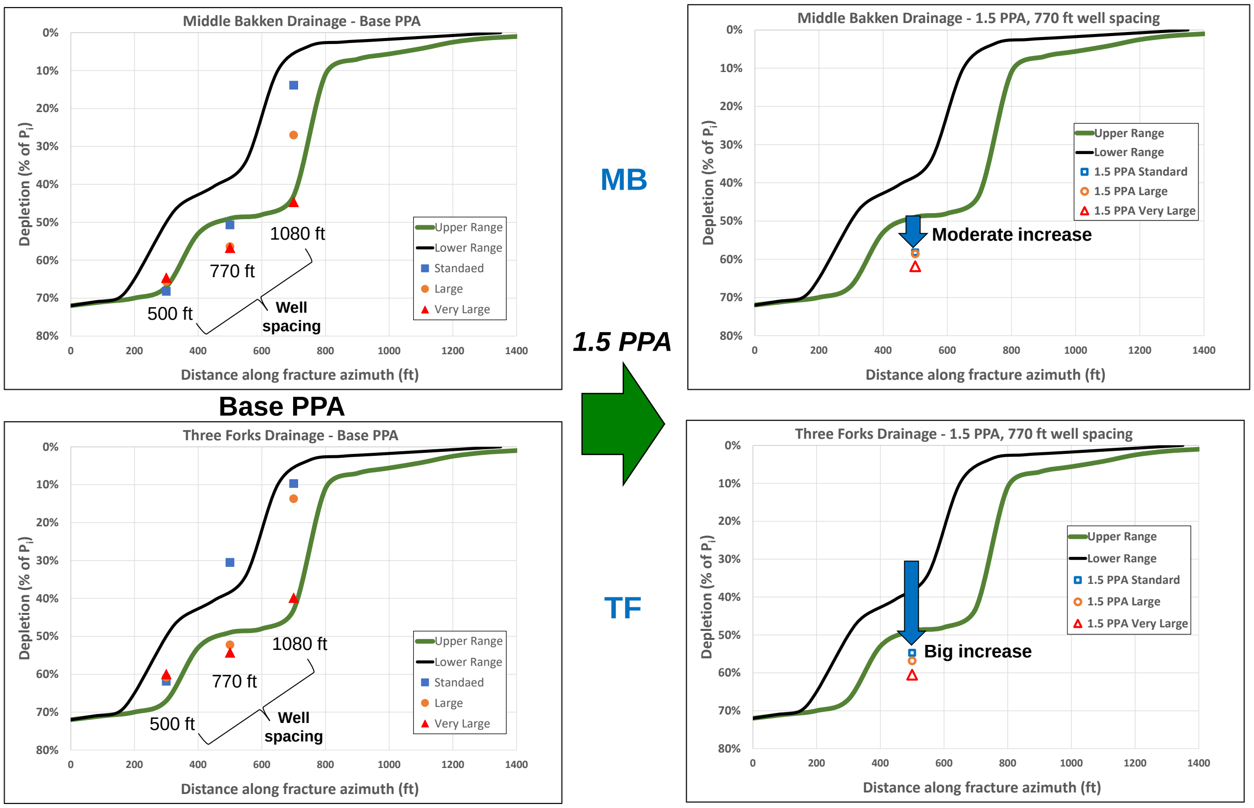

Figure 8 - Drainage efficiency and job size (left), drainage with 1.5 PPA and 770 ft well spacing (right)

Well performance and proppant loading

The effect of proppant loading was evaluated for a 770 ft well spacing and average proppant loadings of 1.2, 1.5, and 2.0 PPA. The percentage increase in first-year cumulative production (IP365) and EUR above the base job designs are shown in **Figure 9**. The results represent the average of the three wells in the model and are biased to the outer well performance (two outer wells, one inner well). The modeling indicates that increasing proppant loading could result in substantial increases in well productivity and oil recovery. For example, increasing proppant loading from 1 PPA in the standard job design to 2 PPA results in a 25%

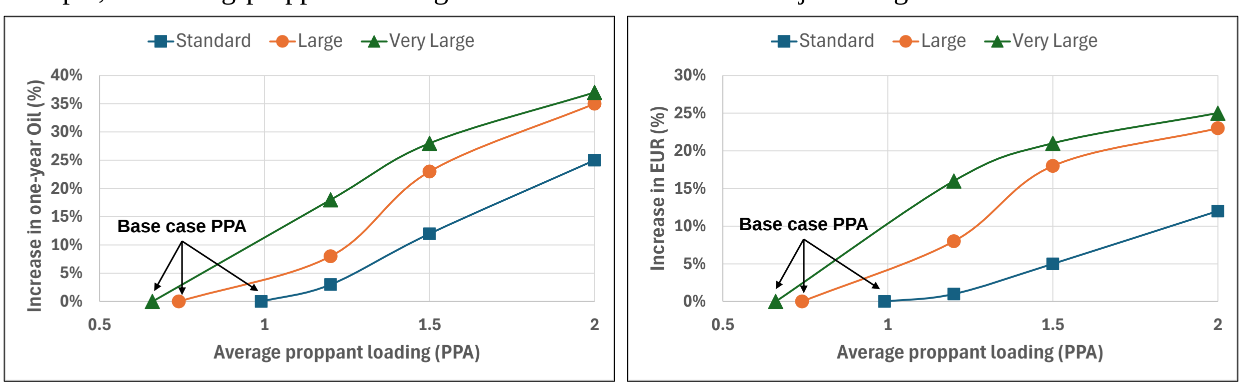

Figure 9 - Well performance, job size, and proppant loading, 770 ft well spacing.

increase in IP365 and a 12% increase in EUR. For the very large job design, increasing proppant loading from the base case of 0.66 PPA to 2 PPA results in a 37% increase in IP365 and a 25% increase in EUR. Due to outer well bias, EUR increases may be optimistic, but the impact of proppant loading on well performance is clear.

The effect of proppant loading and job size on IP365 and EUR are also shown in **Figure 10**, presenting the results for each case (not the % change from the base case). The y-axis scales are masked but still provide a good comparison of well performance. The larger jobs with higher proppant loading provide significantly more initial production and EUR. However, the differences between the three job sizes decreases as proppant loading is increased. Again, the results are biased to the unbounded outer wells that benefit from the increased drainage area with the larger jobs. However, visual inspection of the graphs suggests dimensioning return when job size in increased form large to very large jobs, especially for higher proppant loading of 1.5 to 2.0 PPA.

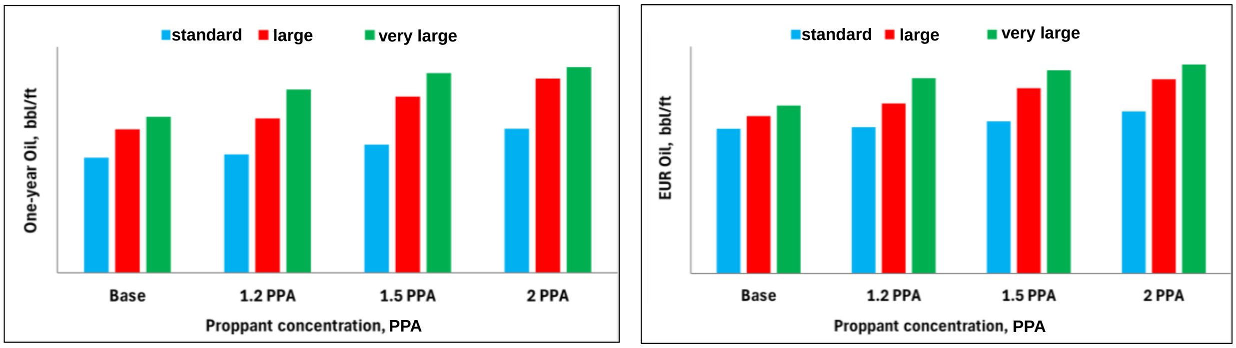

Figure 10 - Effect of proppant loading and job size on IP365 and EUR

This study also included a limited evaluation of the effect if proppant size and scheduling alternatives on well performance. Note that the proppant transport model inputs for 20/40 and 200-mesh sand were not part of the calibration process and are estimates. This evaluation included:

- pumping100% 100 mesh
- pumping 30% 200 mesh, 30% 100 mesh, and 40% 40/70
- leading of 20/40 mesh (10%) with 100 mesh (90%)
- tailing of 20/40 mesh (10%) with 100 mesh (90%)
- lead-in and tail-in of 20/40 mesh (20%) with 100 mesh (80%)
- pumping 20/40 mesh (10%) in between the 100 mesh (90%)
- combo proppant case, 30% 200 mesh and 10% tail-in of 30/50 mesh, 30% 100 mesh, 30% 40/70

Figure 11 compares the above alternative proppant types and schedules using the base case PPA designs as the reference well performance. Pumping 100% 100-mesh proppant results in slightly lower IP365 compared to pumping the based case 50/50 mix of 100-mesh and 40/70 sand. However, using 200-mesh for the initial 30% of the proppant results in a 6% increase in IP365 due to increased propped length (i.e. – smaller proppant is transported farther). Utilizing a small amount larger, more conductive 20/40 sand also increases IP365. The results suggest there could be an opportunity to improve productivity by 6-10% using alternate proppant types and creative proppant schedules. However, there are operational complexities and supply chain issues that make this opportunity less attractive than increasing proppant loading.

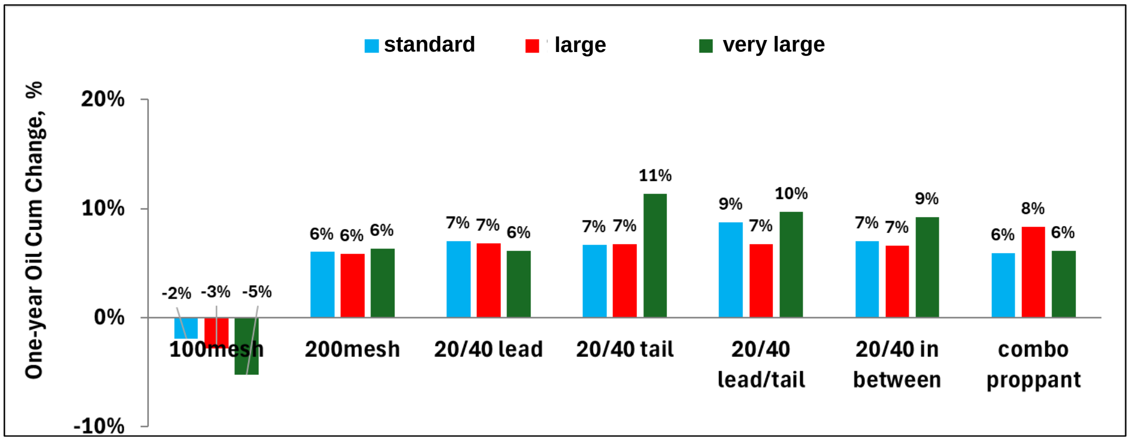

Figure 11 - Evaluation of proppant size and pumping schedules.

Economic comparison
The goal of most optimizations is to maximize value. The modeling indicated a significant opportunity to increase initial production and oil recovery with higher proppant loadings. However, completions costs will be higher due to the substantial increase in proppant pumped and likely increases in friction reducer required to successfully place the higher proppant loadings. Note, fluid volumes for each job size were held constant and the increased proppant volume is achieved by pumping higher proppant concentrations (i.e. - increasing PPA). Although the details of the economic inputs are confidential, typical Bakken drilling, completion, production, and gathering costs and taxes were used in this analysis. **Figure 12** shows the increase in well cost as a function of average proppant loading, as a percentage increase above the base case job design shown in Figure 7. Increasing proppant loading for the standard job design results in a modest increase in well cost, about 8% for a 2 PPA loading, However, increasing proppant loading to 2 PPA for the very large job size results in a 24% increase in well cost.

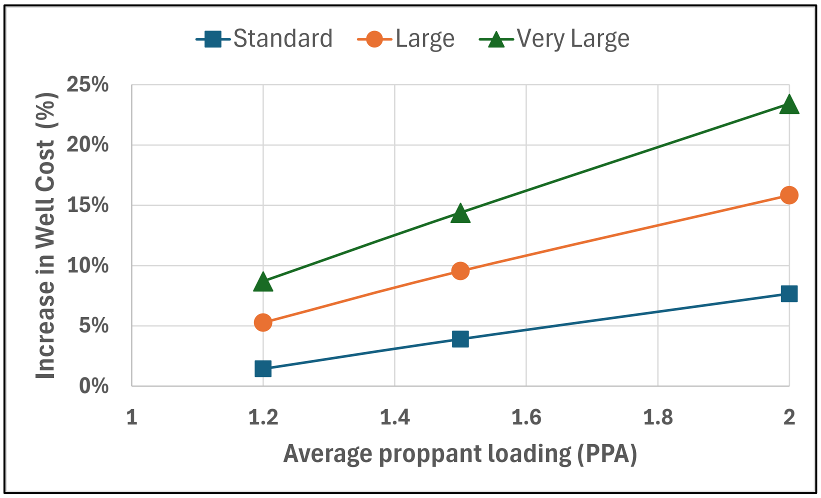

Figure 12 - Percent increase in well cost, above the base case designs (Figure 7), as a function of proppant loading

Oil and gas prices were based on industry forecasts at the time of the study (2024). The economic comparisons are intended to provide insights into the benefit/feasibility of increasing proppant loading and are not intended to be a comprehensive economic optimization. In addition, the optimum job size and proppant will differ depending on well spacing and reservoir quality.

The economic results are presented as incremental, with the base PPA designs as the reference. The economic comparison focuses on the 770 ft well spacing cases (reference Figure 9 and Figure 10). **Figure 13** shows the percent increase in NPV and incremental NPVR (incr. NPV/incr. cost) as a function of proppant loading and job size. NPV can be increased up to 35%, emphasizing the significant economic opportunity that increasing proppant loading presents. Both graphs show a maximum for the large and very large jobs around 1.5 PPA. The standard job size continues to add incremental value up to 2 PPA, while the incremental NPVR decreases slightly compared to the 1.5 PPA design.

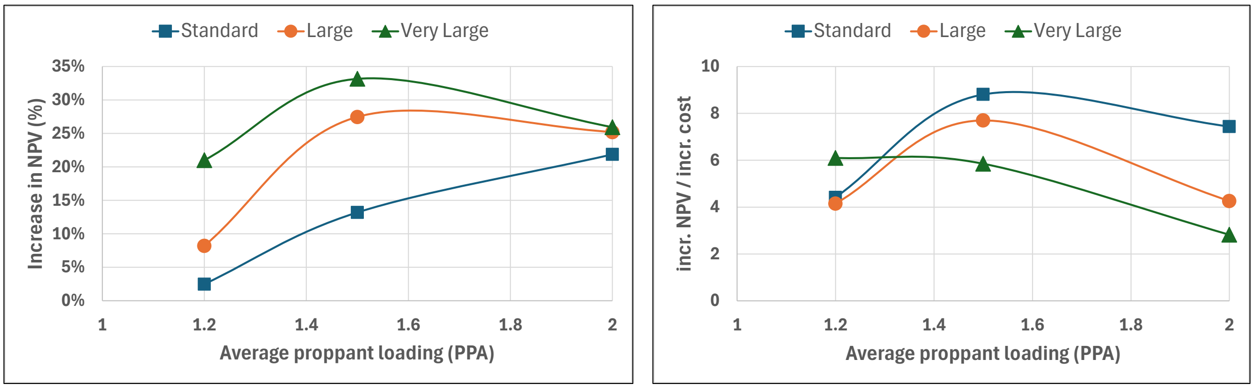

Figure 13 - Economic comparison, percent increase in NPV and incremental NPVR (incr. NPV/incr. cost)

Figure 14 summarizes the economics of the various treatment designs, showing the DROI and NPV/DSU. The highest NPV is predicted for very large fluid volumes and 1.5 PPA average proppant concentration, while the highest DROI is predicted for large fluid volumes and 1.5 PPA.

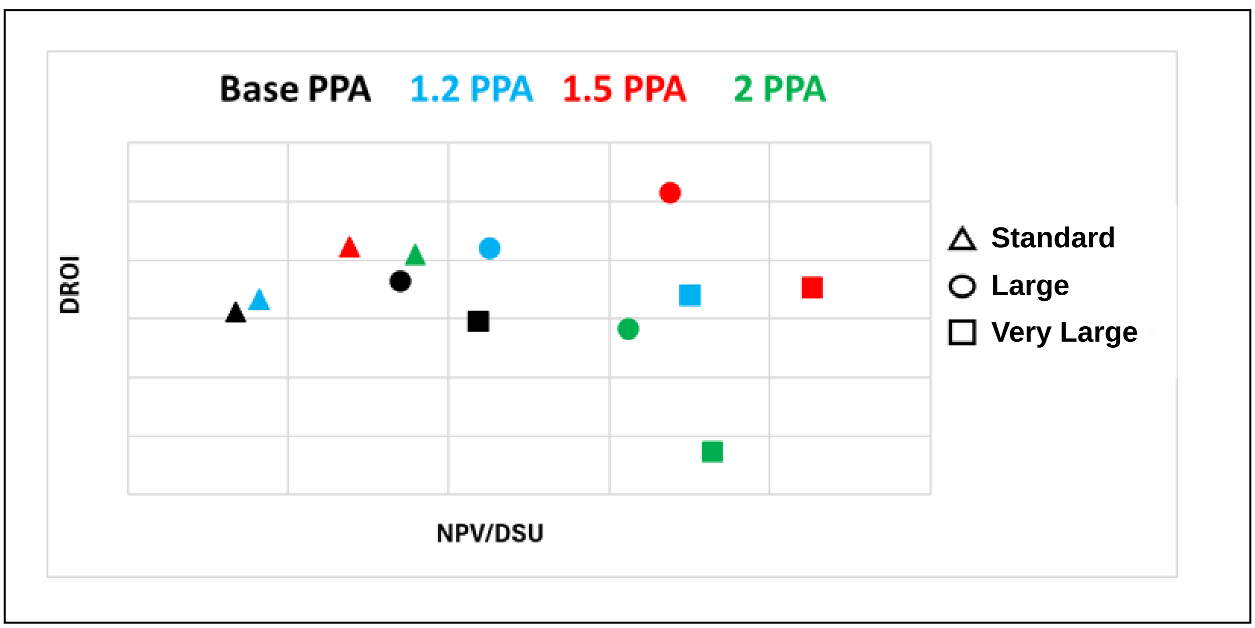

Figure 14 - Discounted return on investment (DROI) and DSU net present value (NPV)

The economic benefits of increasing proppant loading appear to be substantial. Although completion costs increase, the predicted increase in production and EUR result in multi-million dollar increases in value. The DROI and NPV/DSU predictions illustrate the trade-off between maximizing rate of return and NPV, suggesting that for 770 ft well spacing the large to very large treatment volumes with 1.5 PPA may provide the best value. The economics will differ based on each operator's cost structure, contracts, price forecasts, and economic optimization criteria. In the study, incremental NPV and incremental NPV/incremental cost are used to illustrate the potential benefits of increasing proppant loading.

The Way Forward

Completion designs have continually evolved based on learning from the drainage mapping projects (Cipolla et. al. 2022, Liang et. al, 2022, McKimmy et. al. 2025) and field trials. Average proppant loadings have increased from 1.0 PPA in 2022 to 1.3 PPA in 2024, recognizing that increasing fracture conductivity may be a significant economic opportunity. Although a limited number, recent analog comparisons support the model predictions, showing production increases of 5-20% when proppant loading in increased by 0.5 PPA (average PPA of 1.35-1.6). Several trials are planned in 2025 to evaluate proppant loading of 1.8-2 PPA.

The next transformational opportunity is increasing conductivity in the "currently" unproductivity portion of the hydraulic fracture. The drainage measurements show that only about 50% of the created fracture length is productive (i.e. – drainage is limited to the first 50% of the fracture length). And that the unpropped fracture conductivity (UPC) is very low, around 0.0001 md-ft, resulting in only minor drainage (reference Figure 1). **Figure 15** repeats the modeling results for the standard job size and 770 ft well spacing, showing the potential to increase IP365 by 25% with a proppant loading of 2 PPA (base case is 1 PPA). However, if the conductivity of the unpropped region of the fracture can be increased 10x, IP365 and EUR can be increased by over 60%. With a 40x increase in UPC, IP365 increases by 120% and EUR increases by 80%. The implications are transformational, much larger well spacing and more productive wells. Unfortunately, we have not identified or developed the technology to exploit this opportunity.

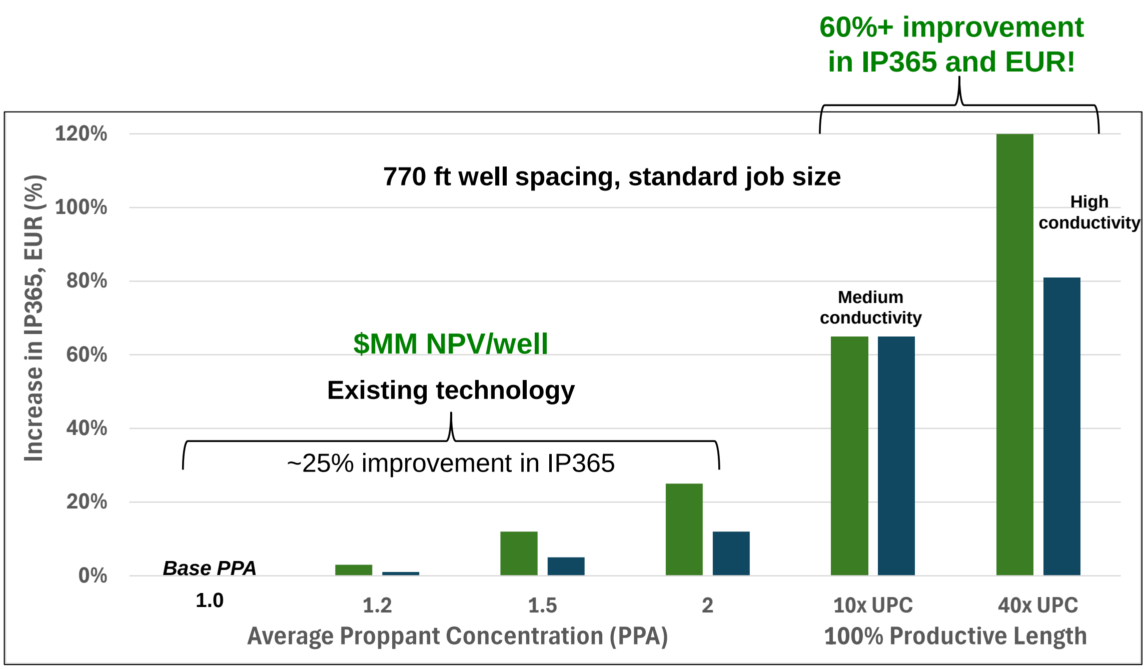

Figure 15 - Transformational opportunity, increasing productive fracture length.

This study included an evaluation of a novel single-well trial design. The study focused on MB-only development and did not include MB-TF development. Single-well trials would reduce costs compared to full-pad trials and allow more trials. The results showed that single-well trials are feasible if designed properly and there were at least five wells on the pad. The details on the single-well trial evaluation and design guideline are provided in **Appendix 1.** Due to uncertainties in bulk-and-test production allocations and difficulty finding pads where the single-well trial criteria could be satisfied, the operator chose to conduct full-pad trials for the initial evaluation study.

Summary and Conclusions

A fully coupled hydraulic fracture and reservoir simulation model was successfully calibrated to match a comprehensive multi-project dataset of diverse measurements, including offset well and completion well fiber optic, microseismic, offset well cemented gauges, perforation imaging, and well performance. The calibrated model was used to evaluate the impact of proppant loading on well performance and drainage efficiency. The results of this work are directional in nature and not intended to be a rigorous optimization, but the results of this work provide important insights:

1. Increasing proppant loading from 1 to 2 PPA for a standard treatment size, may increase well productivity by 25% and EUR by 12%.
2. Increasing proppant loading from 0.74 to 2 PPA for a large treatment size, may increase well productivity by 35% and EUR by 23%.
3. Increasing proppant loading from 0.66 to 2 PPA for a very large treatment size, may increase well productivity by 37% and EUR by 25%.
4. The production and EUR increases are biased toward the performance of the outer, un-bounded wells. The benefits of higher proppants loadings with large and very large jobs sizes reported in this paper are probably more representative of wider well spacing (i.e. – greater than 770 ft) where the increased drainage efficiency of larger jobs sizes can be fully exploited.
5. Predicted drainage efficiency at 770 ft well spacing for the standard job size with 2 PPA proppant loading suggests that modest treatment volumes may be sufficient, highlighting the trade-off between treatment volume and proppant loading.
6. Depending on the economic optimization criteria, large to very large treatment volumes with an average proppant loading of 1.5 PPA may provide best value.
7. Well productivity and drainage may be improved using a wide range of proppant sizes, with smaller proppants used to improve far-field drainage and larger proppants used to increase near and mid-field fracture conductivity.
8. If the production and EUR increases suggested by the modeling can be realized, the economic value is significant.
9. Single-well trials may be feasible if designed properly with 5+ wells per pad.
10. There is a transformational opportunity to fully exploit the total fracture length, with the potential to double productivity and drainage.

Acknowledgements

The authors would like to thank Hess Corporation for supporting the publication of the work and the Hess Bakken team for their support of the data acquisition projects. The authors would also like to thank Khalid Shaarawi, Robert Fast, Erin Shade and Bryan Baca for supporting the Hess fracture conductivity initiative. Special thanks to Hess Leadership for supporting the innovation culture that advanced our understanding of fracture conductivity and drainage in the Bakken.

Disclaimer

Note that neither Hess nor ResFrac makes any representation, express or implied, as to the completeness, accuracy, or adequacy of the information contained herein. Information in the materials can include, but is not limited to, oil and gas production data, lease operating data, flaring forecasts, and other information and forward-looking statements. Forward-looking statements may include, without limitation: future financial or operational results; business strategy; estimates of crude oil and natural gas production and flaring; projected budget and capital and exploratory expenditures; expected timing and completion of development projects; and future economic and market conditions in the oil and gas industry. Caution should be taken not to place undue reliance on any such forward-looking statements because such statements speak only as of the date when made and there can be no assurance that such forward-looking statements will occur. Actual results may differ materially from those contained in any forward-looking statement we make.

Nomenclature

BHP	= bottomhole pressure, F/ L2
Depletion	= $(P_i-P)/P_i$
DSU	= drilling spacing unit
DROI	= discounted return on investment, %
E	= East
EUR	= Estimated Ultimate Recovery
ft	= Feet
IP365	= first year cumulative production, L3
MB	= Middle Bakken
md	= Millidarcy, L2
N	= North
NPV	= Net present value, $
NPVR	= Net present value/cost
P_i	= original reservoir pressure, L3
P	= current pressure, L3
PPA	= total pounds of proppant added per total fluid volume in gallons, M/L3
S	= South
STB	= stock tank barrels
TF	= Three Forks
UPC	= unpropped conductivity, L3
W	= west

SI Metric Conversion Factors

acre	x	4.046 873e+03	=	m^2
bbl	x	1.589 874e-01	=	m^3
cp	x	1.0e-03	=	Pa.s
ft	x	3.048e-01	=	m
°F		(°F – 32)/1.8	=	°C
lbm/gal	x	1.198 264e+02	=	kg/cm^2
psi	x	6.894 757e+00	=	kPa

References

Cipolla, C., Wolters, J., McKimmy, M., Miranda, C., Hari-Roy, S., Kechemir, A., Gupta, N. 2022. "Observation Lateral Project: Direct Measurement of Far-field Drainage." Paper presented at SPE Hydraulic Fracturing Technology Conference and Exhibition, The Woodlands, Texas, USA, February 2022. SPE-209164-MS. https://doi.org/10.2118/209164-PA.

Cipolla, C., Kechemir, A., McKimmy, M., Shaarawi, K., and Fast, R. 2024. "Novel Well Design for Unconventionals: Augmented Drainage Development (ADD)." URTEC-4044110-MS, paper presented at the Unconventional Resources Technology Conference held in Houston, Texas, USA, 17-19 June 2024. https://doi.org/10.15530/urtec-2024-4044110.

Liang, Y., et al. 2022. "Accelerating Development Optimization in the Bakken Using an Integrated Fracture Diagnostic Pilot." URTeC 3719696. Paper presented at the Unconventional Resources Technology Conference held in Houston, Texas, USA, 20-22 June 2022. https://doi.org/10.15530/urtec-2022-3719696.

McClure, M. et al. 2023. "Results from a Collaborative Industry Study on Parent/Child Interactions: Bakken, Permian Basin, and Montney." SPE-212321-MS. Presented at the SPE Hydraulic Fracturing Technology Conference and Exhibition, The Woodlands, Texas, USA, 31 January - 2 February 2023.

McClure, Mark, Charles Kang, Chris Hewson, Soma Medam, Egor Dontsov, Ankush Singh, Carlo Peruzzo, and Elizaveta Gordeliy. 2024a. ResFrac Technical Writeup. 17th Edition. arXiv:1804.02092.

McClure, Mark, Fowler, Garrett, Hewson, Chris, and Charles Kang. 2024b. The A to Z Guide to Accelerating Continuous Improvement with ResFrac. 4th edition. arXiv:2205.14820.

McKimmy, M., Cipolla, C., Miranda, C., Rudolph, S., Shaarawi, K. 2025. "Case History of Drainage Mapping and Infill Well Performance in the Bakken." URTeC 4244595 presented at the SPE/AAPG/SEG Unconventional Resources Technology Conference, Houston, Texas, USA, June 2025

Miranda, C., McKimmy, M., Cipolla, C. 2025. "Analysis of far-field drainage from pilot experiments in the Bakken." URTeC 4199865 presented at the SPE/AAPG/SEG Unconventional Resources Technology Conference, Houston, Texas, USA, June 2025

Msalli, A. and Miskimins, J. 2020. Experimental Quantification of Slickwater Proppant Transport in Subsidiary Hydraulic Fractures. IPTC-20329-MS, presented at the International Petroleum Technology Conference, Dhahran, Kingdom of Saudi Arabia, January 2020. https://doi.org/10.2523/IPTC-20329-MS

Palisch, T., Duenckel, R., Bazan, L, Heidt, H., Turk, G. 2007. ". Determining Realistic Fracture Conductivity and Understanding Its Impact on Well Performance—Theory and Field Examples." SPE 106301, presented at the SPE Hydraulic Fracturing Technology Conference and Exhibition, The Woodlands, Texas, USA, January 2007.

Singh, A. et. al. 2025. "Far-Field Drainage along Hydraulic Fractures: Insights from Integrated Modeling Studies in the Bakken and Permian Basin." SPE-223567-MS, presented at the SPE Hydraulic Fracturing Technology Conference and Exhibition, The Woodlands, Texas, USA, February 2025. https://doi.org/10.2118/223567-MS.

Appendix 1

Due to the inherent variability of well performance in unconventional developments, conducting field trials to evaluate new stimulation designs can be challenging, especially if the production improvements are modest 5-20%. These modest improvements in production can be valuable, but there is typically an increase in cost associated with these improvements and it is important that the production uplift is reliably determined. With multi-well pads the standard for most unconventional development, pad-scale trials are the norm. This requires identifying suitable analog pads to evaluate the trial, which can be difficult given variability in reservoir quality, well spacing, well placement, parent-child interactions, and completion designs. And several pads could be required to ensure the trial is statistically relevant. It would be less expensive and allow more trials if single-well trials are feasible. This work included an evaluation of the feasibility of single-well trials.

A five-well pad was modeled to determine the feasibility of single-well trials, with the focus on evaluating the effect of increasing proppant loading on well performance (**Figure 16**). Well spacing of 770 ft (E-W) was used for the study, consistent with the evaluation of proppant loading presented in Figure 9. The objective was to determine if an offset well can be used as the analog to measure production change. However, nearby wells could be impacted by the trial design, referred to as the system effect. The system effect is an important consideration, as the optimum well spacing typically results in some degree of well-to-well interference. Due to the likely variability of parent-child effects and uncertainty in drainage area, the outer wells were not considered suitable for single-well trials. In addition, due to the likelihood of well-to-well communication, the study focused on interior wells that were separated by a "buffer" well.

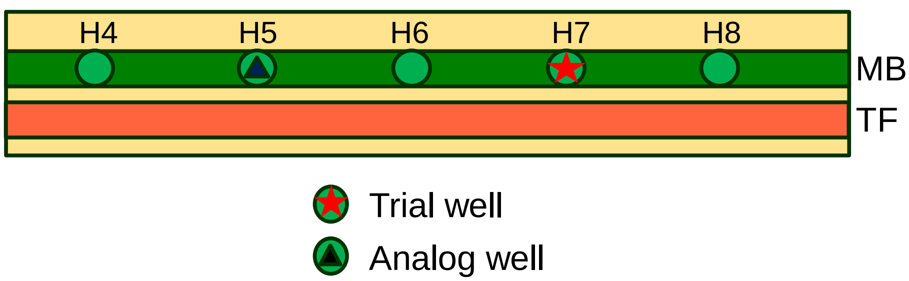

Figure 16 - Five well pad used to study the feasibility of single-well trials.

The single well trial design is shown in Figure 16, with the trial well identified by the red star and the analog well identified by the black triangle. Three simulation cases are modeled to validate the field trial set-up ability to reliable measure the effect of proppant loading on well productivity on a well level:

1. Base design full pad – large job size and 0.74 PPA for all wells (base design)
2. 1.5 PPA full pad – large job size and 1.5 PPA for all wells
3. Trial design – large job size and 0.74 PPA for all wells, **except for 1.5 PPA H7 trial well**

Simulating the production for the full pad base PPA (0.74) and full pad 1.5 PPA case was an important starting point that provided a baseline production uplift (i.e. – if a pad scale trial was performed). Most of the modeling was performed using a three-well model (Figure 7a); this work provides an opportunity to evaluate the impact of outer well bias by comparing the three and five well models. **Figure 17** shows the one-year oil production for each well, comparing the base 0.74 PPA and 1.5 PPA proppant loading. The wells were zippered with the H4, H8, and H6 in the first zipper sequence and the H5 and H7 in the second zipper sequence. The figure highlights the well-to-well variability due to well location (inner versus outer well) and stress shadowing. The first zipper wells are less affected by stress shadowing and out-perform the wells in the second zipper sequence.

The pad-level production comparison shows an 18% uplift using the higher proppant loading of 1.5 PPA. This will be the "expected" uplift to determine if single wells trials are feasible (i.e. – 18% uplift). The three-well model predicted a 23% uplift for this case (Figure 9, large jobs, 1.5 PPA). Although a very limited comparison, as expected the three-well model is somewhat optimistic due to the outer well bias (2:1 ratio of outer to inner wells). The five well model should exhibit less outer well bias (2:3 ratio of outer to inner wells). Although the three-well model outer well bias seems evident, the comparison of the two models supports the overall directionality of the three-well model (i.e. – increasing PPA could materially improve well performance).

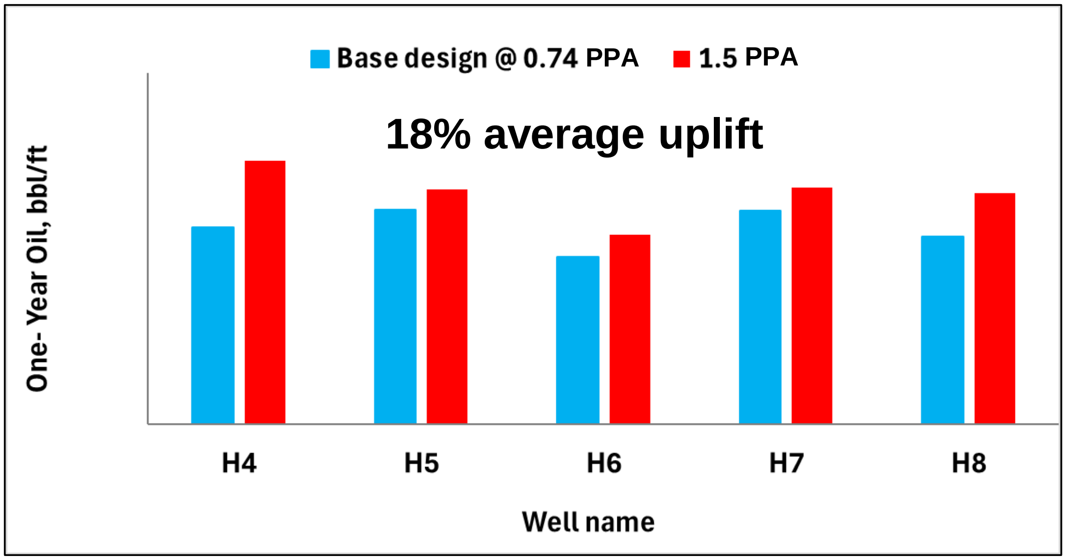

Figure 17 - Comparison of large treatment size at 0.74 PPA (base design) and 1.5 PPA.

The last step in this study was to evaluate the impact of sequencing. Several operational sequences (frac order) were evaluated:

- Frac 1, zipper frac from left to right.
  - 1st zipper - three wells H4, H5, and H6
  - 2nd zipper – two wells H7 and H8

- Frac 2, zipper frac from right to left
  - 1st zipper - three wells H8, H7, and H6
  - 2nd zipper – two wells H5 and H4

- Frac 3, zippering fracs with the following order:
  - 1st zipper - three wells H4, H8, and H6
  - 2nd zipper – two wells H5 and H7

- Simul-frac 1: H4 and H5 first, then H6 and H7, then H8
- Simul-frac 2: H8 and H7 first, then H6 and H5, then H4

The results from the five different frac sequences are summarized in **Figure 18**, illustrating the importance of frac order on the success or failure of a single-well trial. The frac order that shows the expected trial response is Frac 2 & Simul-Frac 2 as the trial well H7 production is approximately 20% higher than H5 analog well. The results showed that zipper frac order should start from the trial well to eliminate any stress shadowing effects on the trial uplift (i.e. - start with H7 & H5 completions). Although the operator decided to implement full-pad trials, single-well trials appear feasible and well be considered for future evaluations.

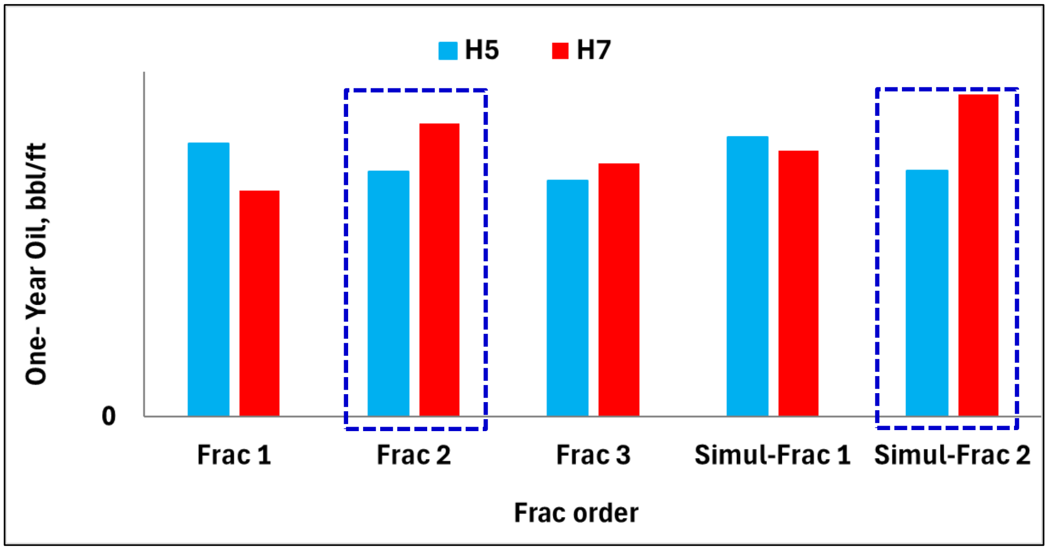

Figure 18 - Effect of frac order on H7 trial well and H5 analog well production.